

Localized Measurement of Strains in Damascene Copper Interconnects by Convergent-Beam Electron Diffraction

Julie A. Nucci¹, Robert R. Keller², Stephan Krämer¹, Cynthia A. Volkert¹, and Mihai E. Gross³

¹Max-Planck-Institut für Metallforschung, Seestraße 92, D-70174 Stuttgart, GERMANY

²N.I.S.T. Materials Reliability Division, 325 Broadway, Boulder, CO 80303, U.S.A.

³Bell Labs, Lucent Technologies, Murray Hill, NJ 07974, U.S.A.

ABSTRACT

Convergent beam electron diffraction (CBED) was used to measure localized lattice strains in damascene copper interconnects. This method provides data from areas of approximate diameter 20 nm, enabling evaluation of strain states within individual grains. Lattice parameters were determined by measuring the deficient higher order Laue zone (HOLZ) line positions in experimental zone axis patterns and subsequently comparing them to kinematical and dynamical simulations. Quantitative comparison was accomplished using a least squares analysis of distances between line intersections. Deposition-induced strains between 0.06% and 0.14% were measured in 2.0 μm wide lines. The uncertainty in strain determination was approximately 0.02%, as limited by the precision in HOLZ line detection. In addition to enabling localized analysis of strain states, another advantage of using CBED is that the microstructure can be fully evaluated. Used in conjunction with global methods such as X-ray diffraction, CBED may provide unique insight into localized failure phenomena such as electromigration void formation in damascene copper.

INTRODUCTION

Several methods are used to measure strains, and hence to infer stresses, in thin films. X-ray diffraction and wafer curvature, which are the most commonly used methods, provide averaged information and result in the determination of a global strain state. Data from such measurements is often correlated to average microstructure, such as texture strength or median grain size. As a result of their global nature, insight into localized phenomena that occur within interconnects is difficult to realize using these approaches. Examples of such localized behavior include electromigration or stress-induced void formation, grain to grain variation in thermal stresses due to elastic anisotropy, and dislocation clustering during plastic deformation in interconnects.

A method being developed for local strain measurement in interconnects is X-ray microdiffraction. Focussed beams of approximate diameter 1 μm [1] were recently produced using this technique. This is sufficient for obtaining strain information from larger individual grains. The main advantage of this technique is that no special specimen preparation techniques are needed; the measured sample strain state represents that of the as-fabricated structure. A disadvantage of this technique is that synchrotron radiation is required to produce such a finely focussed X-ray beam. While it is possible to extract local texture information using this

technique, it is more difficult to select the precise location from which a measurement is taken since the microstructure cannot be imaged with the precision attained by electron microscopy.

Strain can be measured with spatial resolution of approximately 10 nm using convergent-beam electron diffraction (CBED) in a transmission electron microscope (TEM). Since the electron beam can also be used to image the sample, the location from which diffracted information is collected can be precisely selected. This technique was recently applied to measure local strain distributions in free-standing aluminum interconnects. Strain within an individual grain was measured during thermal cycling[2]. Grain-to-grain strain variations were measured in the vicinity of hillocks that formed as a result of electromigration testing [3].

The study of local strain variations is especially relevant to understanding the mechanical properties of copper lines, since strain gradients may produce large stress gradients due to elastic anisotropy. Besides anisotropy, analyzing copper samples requires more careful consideration of dynamical scattering and sample geometry effects, as compared to the analysis of free-standing aluminum lines. We address these issues in this paper and demonstrate the feasibility of measuring strain in sub-micrometer grains from damascene copper lines using CBED.

EXPERIMENTAL

The samples studied were damascene-processed copper lines. A 580 nm thermal oxide was grown on a silicon substrate, followed by a 120 nm Si₃N₄ barrier. Trenches of width 2.0 μm, spacing 2.0 μm, depth 0.5 μm, and length 0.5 mm were formed by reactive ion etching of a subsequent SiO₂ layer. Following deposition of a 50 nm tantalum barrier layer and a 100 nm copper seed layer by physical vapor deposition (as measured in the field between trenches), a 1 μm copper film was electroplated over the structure using a CuSO₄/H₂SO₄ bath containing organic additives for good damascene fill. The samples were chemical mechanically polished after room temperature recrystallization, which was deemed to be complete by focussed ion beam imaging.

Plan-view TEM specimens were prepared by the tripod-polishing method. A very brief (approximately 15-20 s) front-side polish was performed using 0.05 μm colloidal silica to remove any copper oxide. Following the setting of a 3° wedge angle, the silicon was polished parallel to the copper line length using wet diamond-embedded paper with grit sizes ranging from 30 μm to 0.1 μm. A schematic of the TEM sample and a micrograph of the copper microstructure are shown in figure 1. Note the extremely fine structure, including a high density of twins.

CBED was performed in a TEM operating at 120 kV. This voltage produces useful configurations of higher order Laue zone (HOLZ) lines, and it allows for penetration through 150 nm of copper, which was the approximate specimen thickness. The TEM was operated in scanning mode, so that a large, continuously variable convergence angle could be formed [4].

Convergence angles of approximately 1° produced Kossel-Möllendorf conditions. Since the microscope was not equipped with an energy filter, the specimen was cooled to -180°C to improve HOLZ line visibility through suppression of thermal vibrations. The strain associated with this cooling was considered in the final strain analysis.

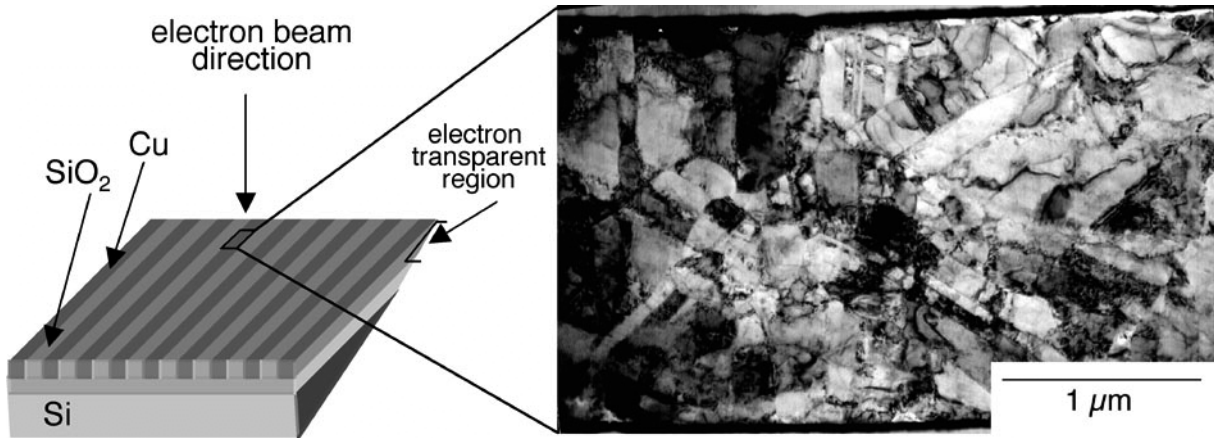


Figure 1. Schematic of specimen geometry and bright-field TEM micrograph showing as-deposited structure.

STRAIN MEASUREMENT BY CBED

CBED patterns are obtained by converging the electron beam into a cone shape. By illuminating the sample with such a beam, a continuous distribution of incident electron directions is produced within the bounds of the cone surface. The diffraction spots formed by parallel illumination become discs when the beam is converged. Under these conditions, each disc is formed since the incident beam directions within the cone simultaneously satisfy a single Bragg condition. The central disc is used for strain analysis.

Dark deficient lines within the central disc result from HOLZ reflections. Since these reflections often have large \mathbf{g} -vectors, the correspondingly high Bragg angle leads to a relatively large shift of the HOLZ lines. In addition, lines become sharper with increasing $|\mathbf{g}|$, so their positions in the pattern become better defined. As a result, lattice distortions can be measured with great sensitivity. Limits to the resolution attainable by CBED depend on the combination of which reflections are present, how sensitive those reflections are to the individual strain components, and how precisely the line positions can be measured. Figure 2 shows how the individual HOLZ line positions shift as a result of a strain applied in the plane normal to the incident beam. Figure 2a and 2b show the HOLZ line shifts induced by applying strain along the x and y directions. Figure 2c was produced by application of a shear strain in the xy plane. In this figure, the x-direction runs horizontally, the y- vertically. Since the HOLZ lines respond differently to the applied strain, multiple strain components can be evaluated by considering a set of HOLZ lines. A single diffraction pattern can provide information about the triaxial strain state since there is also a measurable z-component of the reciprocal lattice vectors.

A recently developed methodology for quantitatively evaluating CBED patterns for strain analysis is detailed in reference 3, and briefly summarized here. Line positions in the experimental pattern are determined using a Hough transform[5], which is well-suited to precisely locating narrow lines of even faint contrast, with sub-pixel precision. The experimental patterns are then compared with simulated kinematic patterns that vary systematically with strain. However, the dynamical interaction between the incident electrons and the crystal potential of copper can result in HOLZ line shifts equivalent to shifts induced by 0.3% strain. Since the dynamical shift can be larger than shifts induced by the experimental strain, this effect

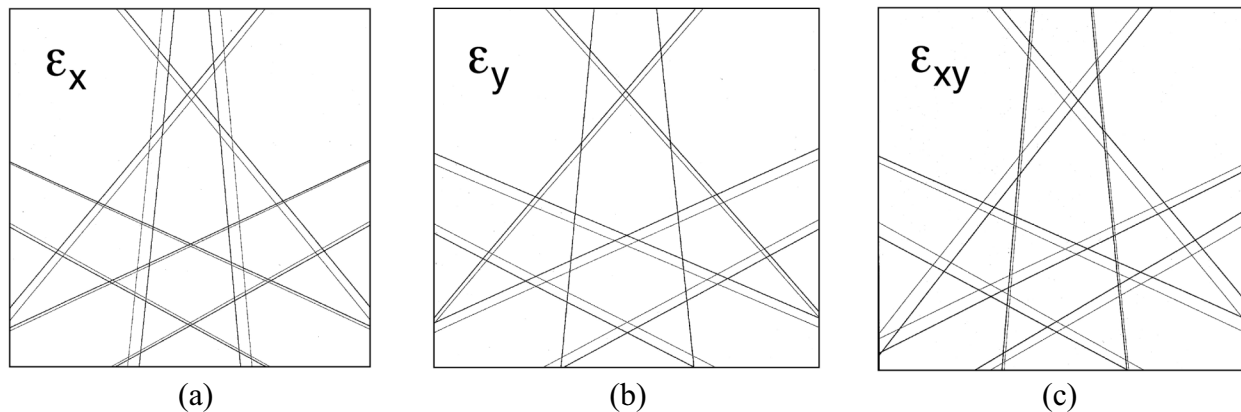


Figure 2. Effect of strain components on HOLZ line positions. x -direction runs horizontally, y -direction runs vertically. Thinner lines represent unstrained state.

must be properly considered. The goodness-of-fit between the theoretical and experimental data is determined by performing a nonlinear least-squares fit analysis using normalized distances between HOLZ line intersections. Standard optimization routines are employed to seek out the best fitting solution.

Multiple combinations of strain components can lead to the same solution. This multiplicity arises since the zone axis patterns display only the deficient lines; an absolute measure of Bragg angles cannot be made. For example, it is possible for a tensile in-plane strain to give rise to the same deficient line position as a compressive out-of-plane strain. A reasonable assumption about the geometry and mechanics of the specimen must therefore be made to eliminate physically non-realistic strain states.

RESULTS AND DISCUSSION

Figure 3 shows a $[233]$ zone axis pattern obtained from a single grain in a copper interconnect, with the specimen held at -180°C . A kinematical simulation is overlaid onto this pattern in the adjacent image. The best-fit simulation was created using lattice constants corresponding to a longitudinal strain $\epsilon_x = 0.16\%$, a transverse strain $\epsilon_y = 0.19\%$, and a normal strain $\epsilon_z = -0.13\%$. These values include the thermal strain (assumed to be elastic) at the low temperature.

Extrapolation of the result back to room temperature was accomplished with the aid of a two-dimensional finite element analysis, in which the thermal strain associated with a 200°C temperature drop from room temperature was modeled in addition to the loss of silicon-induced constraint due to thinning. The plan view TEM geometry was modeled as $5\ \mu\text{m}$ long copper and oxide stripes fixed together and rigidly bound to silicon along their widths at one end of the sample. Only half of the copper and oxide linewidths were meshed, due to symmetry. A plane stress model was used to best approximate the strain state in the TEM sample since relaxation of macroscopic stresses in the z direction is possible. Strains varied greatly within approximately $1\ \mu\text{m}$ of either edge of the line, and were reasonably uniform for the middle $3\ \mu\text{m}$. Within this uniform region, the copper exhibited a longitudinal tensile strain of approximately 0.10% and a

transverse tensile strain of approximately 0.05%, due to the 200°C decrease in temperature. One might be concerned that the copper could undergo plastic deformation upon cooling to -180°C ,

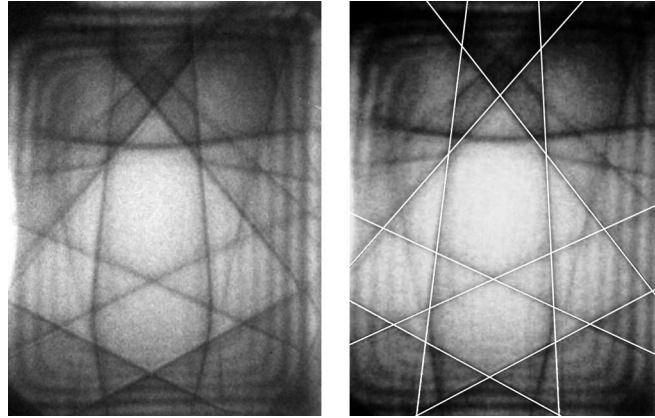


Figure 3. [233] zone axis pattern and same pattern with kinematical simulation overlaid. Pattern obtained from a copper grain, with specimen held at -180°C . Simulation corresponds to $\epsilon_x = 0.16\%$, $\epsilon_y = 0.19\%$ at the low temperature.

since the thermal stress in the thinned specimen is of the order of 190 MPa. The lack of a uniformly high density of dislocations as shown in Figure 1 suggests that this did not occur, perhaps as a result of the extremely fine grain size. Upon subtracting these thermal strains from the strains measured by CBED, we can estimate the in-plane strain state of the specimen prior to cooling, assuming no plastic deformation occurred. The room temperature result is $\epsilon_x = 0.06\%$ and $\epsilon_y = 0.14\%$. We are aware of no other localized strain measurements at this scale, to which we can compare this result.

The uncertainty in the measurement was approximately 0.02% strain. This was limited by the goodness of fit between the experimental line positions and the simulated line positions. Use of an automated Hough transform and polynomial peak-fitting routine resulted in locating HOLZ line positions with an accuracy of approximately 0.2 pixel [2]. Subsequent use of a grid search optimization scheme led to the strain state depicted in figure 3.

Note that specimen thinning affects only a load applied to the original sample macroscopically, such as the strain due to thermal expansion mismatch. Localized sources of strain such as those described in the introduction are not expected to change dramatically upon removal of the silicon substrate. In electroplated copper lines, localized strains are also expected, due to either residual plating compounds in grain boundaries and other defects [6] or to fine scale dislocation substructure formation [7]. We have not specifically identified the localized source in this study.

Work in progress involves use of an energy-filtering TEM, which allows for the acquisition of good quality HOLZ lines at room temperature and above. Room temperature measurement simplifies the analysis since there is no need to consider a thermal strain correction. Ongoing work also involves the preparation of cross sectional TEM specimens using focussed ion beam methods in order to better preserve the bulk strain state. For example, when a very small region of the sample (approximately 20 μm long) is thinned along the length of the line to approximately 120 nm, the small electron transparent region is embedded in a much thicker,

more mechanically stable piece of silicon. Analytical modeling of this sample geometry revealed that the strain along the line length is consistent with that along the line length in the bulk material. Relevant comparisons of the longitudinal strain among adjacent grains can then be made. Such comparisons should provide insight into the nature of the localized stress and strain distributions in damascene lines.

CONCLUSIONS

We have demonstrated the feasibility of using convergent-beam electron diffraction to locally measure strain states in damascene copper lines. Tensile strains between 0.06 and 0.14% were measured, with an uncertainty of 0.02% due to the line detection procedure. This paper addressed some of the issues associated with making measurements of strain using TEM samples. With proper consideration of relaxation due to thinning, reasonable conclusions about the original strain state can be inferred. By suitable combination of X-ray methods with CBED, the global and localized strain states in narrow interconnects can be more quantitatively characterized.

ACKNOWLEDGMENTS

RRK thanks the NIST Office of Microelectronics Programs.

REFERENCES

- 1 . N. Tamura, J. -S. Chung, G. E. Ice, and B. C. Larson in *Materials Reliability in Microelectronics IX*, edited by D. D. Brown, A. H. Verbruggen, and C. A. Volkert (Mater. Res. Soc. Proc. **563**, Pittsburgh, PA, 1999) pp. 175-180.
- 2 . S. Krämer, J. Mayer, *Proc. Fifth Int'l Workshop on Stress-Induced Phenomena in Metallization*, edited by O. Kraft, E. Arzt, C. A. Volkert, P. S. Ho, and H. Okabayashi (AIP Conf. Proc. 491, New York, 1999), pp. 289-297.
- 3 . S. Krämer, J. Mayer, C. Witt, A. Weickenmeier and M. Rühle, "Analysis of local strain in aluminium interconnects by energy-filtered CBED", *Ultramicroscopy*. **81**, in press (2000).
- 4 . D. B. Williams, *Practical Analytical Electron Microscopy in Materials Science* (Philips Electronic Instruments, Deerfield Beach, FL, 1984), p. 125.
- 5 . Hough, P. V. C., U.S. Patent 3,069,654 (1962).
- 6 . S. H. Brongersma, E. Richard, I. Vervoort, and K. Maex, in *Proc. Fifth Int'l Workshop on Stress-Induced Phenomena in Metallization*, edited by O. Kraft, E. Arzt, C. A. Volkert, P. S. Ho, and H. Okabayashi (AIP Conf. Proc. 491, New York, 1999), pp. 249-254.
- 7 . C. Cabral, Jr., P. C. Andricacos, L. Gignac, I. C. Noyan, K. P. Rodbell, T. M. Shaw, R. Rosenberg, J. M. E. Harper, P. W. DeHaven, P. S. Locke, S. Malhotra, C. Uzoh, and S. J. Klepeis, in *Proc. Advanced Metallization Conference in 1998*, edited by G. S. Sandhu, H. Koerner, M. Murakami, U. Yasuda, and N. Kobayashi (Mater. Res. Soc., Pittsburgh, PA, 1999), pp. 81-87.